

---

**Pacific Northwest  
National Laboratory**

Operated by Battelle for the  
U.S. Department of Energy

# Feasibility Study of Using Short Wave Infrared Cavity Ringdown Spectroscopy (SWIR-CRDS) for Biological Agent Detection

PM Aker      RM Williams  
TJ Johnson    NB Valentine

October 2007

Prepared for the U.S. Department of Energy  
under Contract DE-AC05-76RL01830



## DISCLAIMER

This report was prepared as an account of work sponsored by an agency of the United States Government. Neither the United States Government nor any agency thereof, nor Battelle Memorial Institute, nor any of their employees, makes **any warranty, express or implied, or assumes any legal liability or responsibility for the accuracy, completeness, or usefulness of any information, apparatus, product, or process disclosed, or represents that its use would not infringe privately owned rights.** Reference herein to any specific commercial product, process, or service by trade name, trademark, manufacturer, or otherwise does not necessarily constitute or imply its endorsement, recommendation, or favoring by the United States Government or any agency thereof, or Battelle Memorial Institute. The views and opinions of authors expressed herein do not necessarily state or reflect those of the United States Government or any agency thereof.

PACIFIC NORTHWEST NATIONAL LABORATORY

*operated by*

BATTELLE

*for the*

UNITED STATES DEPARTMENT OF ENERGY

*under Contract DE-AC05-76RL01830*

Printed in the United States of America

Available to DOE and DOE contractors from the  
Office of Scientific and Technical Information,  
P.O. Box 62, Oak Ridge, TN 37831-0062;  
ph: (865) 576-8401  
fax: (865) 576-5728  
email: reports@adonis.osti.gov

Available to the public from the National Technical Information Service,  
U.S. Department of Commerce, 5285 Port Royal Rd., Springfield, VA 22161  
ph: (800) 553-6847  
fax: (703) 605-6900  
email: orders@ntis.fedworld.gov  
online ordering: <http://www.ntis.gov/ordering.htm>



This document was printed on recycled paper.

(9/2003)

# Feasibility Study of Using Short Wave Infrared Cavity Ringdown Spectroscopy (SWIR-CRDS) for Biological Agent Detection

PM Aker      RM Williams  
TJ Johnson    NB Valentine

October 2007

Prepared for the U.S. Department of Energy  
under Contract DE-AC05-76RL01830

# Final Report for Project # 49284

## Feasibility Study of Using Short Wave Infrared Cavity Ring Down Spectroscopy (SWIR-CRDS) for Biological Agent Detection

Pamela Aker, Tim Johnson, Richard Williams and Nancy Valentine  
National Security Directorate, Pacific Northwest National Laboratory  
P.O. Box 999, Mailstop K5-25, Richland, WA 99352

### 1. Executive Summary

This project focused on determining the feasibility of using short wave infrared (SWIR) cavity ring down spectroscopy (CRDS) as a means for real-time detection of biological aerosols.

The first part of the project involved identifying biological agent signatures that could be detected with SWIR CRDS. After an exhaustive search of the open literature it was determined that whole biological spores and/or cells would not be good candidates for direct SWIR CRDS probing because they have no unique SWIR signatures. It was postulated that while whole cells or spores are not good candidates for SWIR CRDS detection, their pyrolysis break-down products might be. A literature search was then conducted to find biological pyrolysis products with low molecular weights and high symmetry since these species most likely would have overtone and combination vibrational bands that can be detected in the SWIR. It was determined that pyrrole, pyridine and picolinamide were good candidates for evaluation. These molecules are formed when proteins and porphyrins, proteins and dipicolinic acid, and dipicolinic acid are pyrolyzed, respectively.

The second part of the project involved measuring quantitative SWIR spectra of pyrrole, pyridine and picolinamide in PNNL's FTIR Spectroscopy Laboratory. Spectral information about these molecules, in the vapor phase is sparse – there were only a few prior studies that measured line positions and no information on absorption cross sections. Absorption cross sections are needed in order to estimate the SWIR CRDS detection sensitivity, and line position determines what type of laser will be needed for the sensor.

The results of the spectroscopy studies allowed us to estimate the SWIR CRDS detection sensitivity for pyrrole to be  $3 \times 10^{12}$  molec  $\text{cm}^{-3}$  or 0.1 ppmv, and for pyridine it was  $1.5 \times 10^{15}$  molec  $\text{cm}^{-3}$  or 0.6 ppmv. These detection sensitivity limits are close what we have measured for ammonia. Given these detection limits we then estimated the amount of biological material that would have to be collected for analysis in a sensor that combined pyrolysis with SWIR CRDS. Using conservative estimates of pyrolysis yields and precursor species concentration we determined that it would be necessary to collect and pyrolyze biological aerosol samples in the 10's of mg. This is a large amount and is far larger than required for current sensors. It is therefore concluded that while possible, the large amounts of material required preclude using SWIR CRDS for detecting biological agents at this time.

## 2. Table of Contents

1. Executive Summary	1
2. Table of Contents	2
3. Introduction	3
4. Survey for SWIR Signatures of Biological Agent Aerosols	4
5. Feasibility of Using SWIR CRDS to Detect Biological Agent Pyrolysis Products	4
6. SWIR Spectroscopy Studies of Gas Phase Pyrrole, Pyridine and Picolinamide	5
6.1 Experimental	6
6.2 SWIR Spectroscopy Results	7
6.3 Estimated SWIR CRDS Detection Sensitivity for Pyrrole and Pyridine Biomarkers	10
7.0 SWIR CRDS Feasibility for Detection Biological Agent Pyrolysis Products	11
8.0 References	12

### 3. Introduction

The real threat of terrorists or hostile nations using biological agents, such as anthrax or smallpox, to attack US interests has emphasized the need for developing new biological sensors and biodetection technologies. This has provided the scientific community with a daunting challenge. Because biological agents can be effective in low doses, biological sensors and detection systems must have high detection sensitivity. The large array of environmental backgrounds against which detection must take place also means that the sensors or systems need to be highly selective (i.e. very low false alarm rate). And to best mitigate the extent of a biological attack, the sensor or system should be capable of real-time detection, or at least have a sampling/analysis time that is on the order of minutes, as opposed to hours or days. Also taken into consideration is the amount of consumables and power required by the sensor and its cost – with the goal being to minimize these parameters.

Considerable progress has been made in the last few years in developing new biosensors and technologies<sup>1, 2</sup> and first generation biological aerosol sensing systems have been field tested.<sup>3</sup> There is still room for improvement however. The requirements of high sensitivity, high selectivity and short analysis time are orthogonal to each other, at least with respect to practical sensor design. As a result it has been decided that the best approach is to combine two or more vastly differing sensing technologies on one platform. The choice of the sensing technologies used depends upon the attack scenario (i.e. will the attack be on a particular food or drinking water supply chain, or will biological aerosols be dispersed over a local area), the method of detection (i.e. point or remote monitoring capability), and also upon the information that is needed from the sensor (i.e. detect-to-warn versus detect-to-treat).

This project is concerned with point detection of biological agent aerosols and more specifically determining if short wave infrared (SWIR) cavity ring-down spectroscopy (CRDS) has the potential to be used in a detect-to-warn strategy. In this case, the sensor platform must be capable of screening an aerosol sample to a) determine if it contains biological material, and b) decide if the biological material represents a threat.

CRDS has previously been used to study systems that mimic, or systems that use, atmospheric aerosols.<sup>4 – 11</sup> These experiments have typically involved measuring particulate extinction (absorption plus scattering) coefficients at one or two laser wavelengths. Experiments have been done using light ranging from the visible into the SWIR, and extinction detection sensitivities in the  $10^{-6} - 10^{-8} \text{ m}^{-1}$  range reported<sup>6-8</sup> – which corresponds, roughly, to mass concentration changes in the  $1 - 10 \mu\text{g m}^{-3}$  range.<sup>8</sup>

The Paldus group has recently reported using CRDS to measure extinction and spectrally resolved fluorescence (in two 100 nm wide bands) of specially doped micro-spheres using 488 nm excitation light.<sup>12</sup> Their observations led them to suggest that different biological aerosols could be differentiated by monitoring the fluorescence spectra. However it is not clear that this CRDS detection approach is viable given the recent observations that the fluorescence spectra seen from a variety of natural biological aerosols and bioagent aerosols are quite similar and, in addition, are highly sensitive to the conditions that the biological species were in while they were growing.

The Schechter group has recently reported measuring broadband CRDS spectra of laser dye-doped aerosols.<sup>11</sup> This result suggests that it may be possible to use tuned laser CRDS to spectrally monitor absorption in biological aerosols and distinguish between biological agents and natural species. Given this, the first focus of this project was to determine if there were any specific SWIR spectroscopic signatures that could be used to distinguish bioagent aerosols from

natural biological aerosols (such as pollen or non-toxic bacterial spores) and ambient aerosol species (such as sulfate or soot aerosols).

#### **4. Survey for Short Wave Infrared (SWIR) Signatures of Biological Agent Aerosols.**

Fourier transform infrared spectroscopy (FTIR) in the long wave infrared region (typically 600 – 4000  $\text{cm}^{-1}$ ) has been used to monitor and distinguish biological material. The work of the Naumann<sup>13</sup> and Goodacre<sup>14</sup> groups in particular has led to major advances understanding the spectroscopy of pathogenic microorganisms. PNNL has also done high quality quantitative spectroscopic studies on several different *Bacillus* strains in both vegetative and sporulated forms. PNNL determined that a straightforward analysis of the transmission spectra at 1070 and 1230  $\text{cm}^{-1}$  could be used to differentiate vegetative bacteria from sporulated bacteria; and that different strains could be identified by comparing second-derivative spectra using a six component principal analysis.<sup>15</sup> PNNL has also demonstrated that second derivative photoacoustic FTIR spectra can also be used to speciate bacterial spores.<sup>16</sup> Several other groups have also reported using long wave FTIR for monitoring whole cells during bioprocessing<sup>17</sup>, and for determining LWIR optical (absorption and/or extinction) cross sections and other optical properties.<sup>18,19</sup>

Given that whole bacterial species have characteristic LWIR signatures, and that SWIR spectroscopy is routinely used to monitor food and drug processing and production,<sup>20</sup> it is not unreasonable to speculate that whole cell signatures might also be present in the SWIR. However, after an exhaustive search of the open literature, it was determined that whole biological spores and/or cells would not be good candidates for direct SWIR CRDS probing because they have no unique SWIR signatures. SWIR spectroscopic studies on *Erwinia herbicola* bacteria and *Bacillus subtilis* spores show that absorption in the 1.0 – 2.5  $\mu\text{m}$  region is flat and contains no unique identifying peaks.<sup>21,22</sup> A comparison of the second derivative spectra in the 2.2 -2.5  $\mu\text{m}$  region of aqueous solutions of several strains of E. Coli and Listeria innocua show some differences.<sup>22</sup> However, this region corresponds to fundamental CH and methylene stretch modes that are present in every biological or organic system, so this region is going to be subject to considerable background interference. It is also worth noting that tunable lasers are not currently available for this spectral region.

#### **5. Feasibility of Using SWIR CRDS to Detect Biological Agent Pyrolysis Products**

While whole cells or spores are not good candidate species for detection using SWIR CRDS, their pyrolysis break down products might be. The genesis for this idea comes from the considerable amount of research that has gone into developing small form factor bioagent detectors - devices which combine pyrolysis with gas chromatography, ion mobility spectroscopy, or compact mass spectrometry.

Thermal pyrolysis has been found to be a viable method for the production of biological markers from whole microorganisms,<sup>23</sup> and several groups have demonstrated that unique biomarkers are associated with bacteria and bacterial spore pyrolysis.<sup>24-40</sup> Some of the products have extremely high molecular weight, but there are also a number of low molecular weight, high volatility species that are produced. As would be expected, the lower molecular weight species prevail when the pyrolysis temperature is high and the residence time is long.

While varied, the main chemical components of cells are macromolecules made up of four classes of monomers – sugars, fatty acids, nucleotides, and amino acids (monomeric constituents of proteins). Sugars (carbohydrates) combine into long polymers called polysaccharides. Cell walls are composed of polysaccharides. Phospholipids play a major structural role in the cytoplasmic membrane.<sup>41</sup> Bacterial spores are composed of the exosporium (multilayered, found in *B. cereus*, *B. thuringiensis* and *B. anthracis*), the spore coat (inner coat and outer coat), the cortex, DNA, and ribosomes.<sup>42-47</sup> The exosporium which protects the spores from chemical and environmental attack consists of several amino acids, lipids, sugars, glucosamine, phosphate, RNA and degraded carbohydrates. The spore coat, which comprises about 50% of the spore's volume, is comprised of many layers with up to 25 cross-linked polypeptide species. Proteins, especially amino acids rich in tyrosine and cysteine are the main constituent of the spore coat, but small amounts of carbohydrates and lipids are also present. The cortex is composed of peptidoglycan which consists of long chains of glycan cross-linked with fragments of peptides.

Simmonds et al. have assigned pyrolysis products from *Bacillus subtilis* and *Micrococcus luteus* to biological classes.<sup>23</sup> They note that pyridine is a product of protein and nucleic acid pyrolysis, while pyrrole is a product of protein and porphyrin pyrolysis. Pyridine is also a thermal degradation product of dipicolinic acid (DPA) which is found in bacterial spores but not in vegetative cells. Pyridine is a small organic molecule that has significant use in the chemical and pharmaceutical industries however – therefore it is a common background interferent so its presence is not a definitive marker for spores. However observation of pyrrole together with pyridine will confirm that species undergoing pyrolysis are biological in character. Picolinamide is a primary product of DPA pyrolysis – its presence along with pyridine and pyrrole will be a key indicator of gram-positive bacteria and/or spores.

Since pyridine, pyrrole and picolinamide have low molecular weight and a fair degree of symmetry we expect that they will have overtone and combination bands that lend themselves amenable to detection with SWIR CRDS. To determine the feasibility of this detection strategy, quantitative measurements of these species SWIR spectra need to be made, since this information is not available. It is to be noted that pyridine, pyrrole and picolinamide are not the only, nor perhaps not the best, bacterial pyrolysis biomarkers. They have been chosen primarily because they contribute appreciably to the pyrolysis yield (under certain conditions) and may have measurable N-H overtone spectra that can be used for species discrimination (note they may show C-H overtones but this is not unique since most other pyrolysis products will be comprised of CH moieties).

## **6. SWIR Spectroscopy Studies of Gas Phase Pyrrole, Pyridine and Picolinamide.**

To determine the feasibility of using SWIR CRDS to detect pyrolysis biomarkers it is necessary that a) the spectra in the SWIR be known in order to determine the wavelength and spread of the laser needed for CRDS measurements, and b) the absorption cross sections (or alternatively transition line strengths) be known to determine if the SWIR CRDS technique is sensitive enough to detect the low concentrations of species that are expected to come from pyrolyzing a small amount of suspect biological material.

An extensive search of the literature revealed that limited information is available about the overtone vibrational transitions of pyrrole and pyridine and nothing for picolinamide. Kjaergaard et al. have measured room temperature pyridine CH stretching overtones in the visible region (500 – 900 nm) in both vapor and liquid phases using intracavity laser



photoacoustic and conventional absorption spectroscopies.<sup>48</sup> They assigned the observed peaks by comparing the experimental results with ab initio calculated bond lengths and they report theoretical and experimentally measured oscillator strengths. More recently McNesby et al. used SWIR FTIR spectroscopy to measure vapor phase pyridine broadband absorption between 1.62 – 1.70  $\mu\text{m}$  (peak at  $\sim 1.67 \mu\text{m}$ ), and then did a narrow band diode laser differential absorption measurement to obtain an absorption cross section of  $3.6 \times 10^{-22} \text{ cm}^2/\text{molecule}$  at 1.63  $\mu\text{m}$ .<sup>49</sup> They did not identify the transition they accessed however. Mellouki et al.<sup>50</sup>, Held and Herman,<sup>60</sup> and Douketis and Reilley,<sup>61</sup> have reported measuring pyrrole N-H overtones in regions from the visible to the long wave infrared fundamental.<sup>50</sup> The first N-H overtone is centered around 1.44  $\mu\text{m}$ . No information was given with regard to line strengths or absorption cross sections.

## 6.1 Experimental

Quantitative near-infrared cross-sections were determined using a slight variant of the method of Chu et al.<sup>50</sup> and Sharpe et al.<sup>51</sup> In this method, a series of Fourier transform IR measurements is made, each corresponding to a different mixing ratio of the pure analyte vapor in a stream of ultra-high purity (UHP) nitrogen gas. After the measurements, a composite absorption spectrum  $A(\lambda)$  is generated from the individual spectrum; the individual (298.1 K) measurements cover a large range ( $\sim 2$  orders of magnitude) of analyte burdens, each burden pressurized with  $\text{N}_2$  to one atmosphere. The fit is derived by generating a Beer's law plot at each wavelength channel to the individual burdens. However, in order to account for various nonlinearity effects in the  $A = f(P)$  fit, the y-axis intensity values in each spectrum are weighted proportional to  $T^2$  (where  $T = I/I_0$ ). All absorbance values  $A > 1.6$  (that is  $T < 0.025$ ) are simply weighted with zero. This multiple burden method greatly improves the S/N ratio by using the high burden measurements to enhance the signal for the weak bands that might not exceed the noise floor in any given measurement (while down-weighting the nonlinear strong peaks), but also using the low burden measurements to bring out a better fidelity for the strong peaks by accounting for Beer's law saturation and detector nonlinearity effects. Chu et al.<sup>51</sup> and Sharpe et al.<sup>52</sup> have demonstrated the advantages of this method compared to a simple linear absorbance data fit at each wavelength bin, since the raw data also have a weighting factor to account for nonlinearity mechanisms. In this method the residual fit vector is, moreover, carefully analyzed since any chemical impurities, including the uncommon ones, readily manifest themselves in the fit residual. The resulting error analysis (Sharpe<sup>53</sup>) shows that the maximal expected systematic errors in absorbance are 3% for the PNNL static-system measurements and 7% for flow-system measurements, including the near-IR values of this work. Random values are less than this, and these results have been vetted against NIST for a host of different molecules as described by Sharpe et al.<sup>52,53</sup> and Johnson et al.<sup>54</sup>, which contain further details of the error analysis.

The three chemicals whose spectra are presented here were purchased as neat liquids from Aldrich Chemical with reported purities of 99.9%, 99.8% and 98% for chloroform, pyridine and pyrrole, respectively. Chloroform is not a potential biomarker species; we have used it in these studies to ascertain the validity of our spectroscopic measurements since its SWIR spectrum has been measured by other groups. The liquids were introduced into the PNNL flow system via a Hamilton 500  $\mu\text{l}$  syringe whose plunger was depressed at a constant rate by a Harvard Apparatus lead-screw driven constant flow syringe pump as given previously by Johnson et al.<sup>54</sup> The spectrometer and White cell arrangement were also re-designed to accommodate a better

thermostatted measurement, as well as to redress known artifacts such as the “warm aperture” problem (Johns et al.<sup>55</sup>, Birk et al.<sup>56</sup>, and Johnson et al.<sup>57</sup>) and detector nonlinearity (Sharpe et al.<sup>52</sup>, Birk et al.<sup>56</sup>). Due to the weaker cross sections in the near-infrared, the White cell path length was increased to 14.52 m ( $\pm 0.5\%$ ). Other general experimental description can be found in Johnson et al.<sup>54</sup>, Masiello et al.<sup>58</sup> and Johnson, Sharpe et al.<sup>59</sup> (2005). The only adaptations to the experiment to convert for near-infrared vapor-phase measurements involved alternate optical components on the Bruker IFS 66v/S to improve the NIR signal/noise: A near-infrared quartz beamsplitter and W-lamp source were employed, as well as a photovoltaic InSb detector. The mirror scan speed was adjusted to 20 kHz, but all other collection parameters were as for the mid-infrared measurements (Sharpe et al.<sup>52</sup>). The NIR spectra covered the 2,700 to 11,000  $\text{cm}^{-1}$  range, for a total range of 550-11,000  $\text{cm}^{-1}$ . Data is only plotted to  $\sim 7,000 \text{ cm}^{-1}$  due to the limited number of bands at higher frequencies.

Picolinamide was purchased as a solid from Aldrich Chemical with a reported purity > 98%. It was dissolved in research grade  $\text{CS}_2$  and the resulting solution injected into the spectrometer as described above. Because the temperature was around 25 °C the picolinamide condensed on the spectrometer cell walls and windows. High quality spectra could therefore not be collected. It may be possible to get high quality data by increasing the spectrometer internal temperature to 60 °C. Budget limitations precluded us from doing these experiments on this project.

## 6.2 SWIR Spectroscopy Results

Figure 1 reports the quantitative near-IR spectra of chloroform, pyridine and pyrrole; the upper two spectra have been vertically offset for clarity by  $5 \times 10^{-6}$  and  $10 \times 10^{-6}$ , respectively. The data are quantitative as each represents a concentration-path burden of 1 ppm-meter. The y-axis has been multiplied by  $10^5$  such that, for example, the 7,127.98  $\text{cm}^{-1}$  peak of chloroform has an absorbance of  $1.34 \times 10^{-6}$  for mixing ratio of 1 ppm through an optical path of 1 m. The raw data have been used to form a composite quantitative fit (Sharpe et al.<sup>52</sup> and Johnson et al.<sup>54</sup>). The only other manipulation was to subtract trace amounts of  $\text{H}_2\text{O}$  vapor from the spectrum and also subtract a small but broad feature due to condensed ice on the detector near 3100-3300  $\text{cm}^{-1}$ . The spectra are all pressure broadened to 760 Torr (high purity  $\text{N}_2$  ballast gas) yet still display several resolved ro-vibronic peaks as detailed below.

Several peaks are of note, but we focus primarily on those that suggest themselves for trace detection using SWIR laser spectroscopy. In general, the C-H stretching region (2,800 - 3,100  $\text{cm}^{-1}$ ) often has strong bands, but only the narrowest of peaks provide any specificity; broad peaks are susceptible to interferences since almost all organic species absorb at these wavelengths.

The bottom trace in Figure 1 is the near-IR spectrum of pyrrole. Pyrrole,  $\text{C}_4\text{H}_5\text{N}$  is a planar aromatic heterocycle of  $\text{C}_{2v}$  symmetry. Its quantitative near-infrared spectrum is reported for the first time in Figure 1. The C-H peaks near 3100  $\text{cm}^{-1}$  have been reported as a composite of three of the four C-H stretching fundamental bands, namely  $\nu_{12}$ ,  $\nu_2$  and  $\nu_{13}$ :<sup>60</sup> These bands are resolved at low pressure and have been assigned,<sup>60,61</sup> but are not resolved in Figure 1 since the spectrum was taken at 760 Torr. The C-H peaks of the first overtone show up around 6150  $\text{cm}^{-1}$  in Figure 2. These have also been previously assigned. In terms of SWIR CRDS monitoring the peak that offers the most promise is the first overtone ( $2\nu_{24}$ ) of the N-H stretch made at 6924.29  $\text{cm}^{-1}$ . It has A1 symmetry – i.e. there are a-type bands with a resolved Q-branch. These features

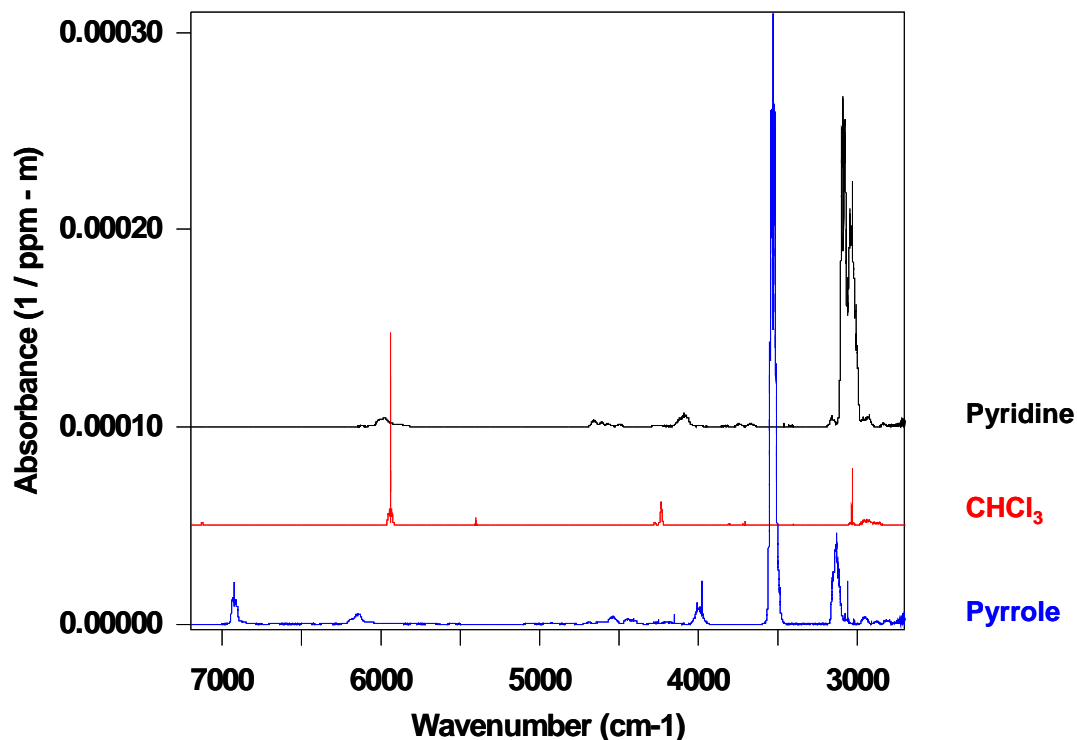


Figure 1. Measured FTIR spectra of vapor phase pyridine, chloroform and pyrrole. Spectra were taken at 760 Torr total pressure.

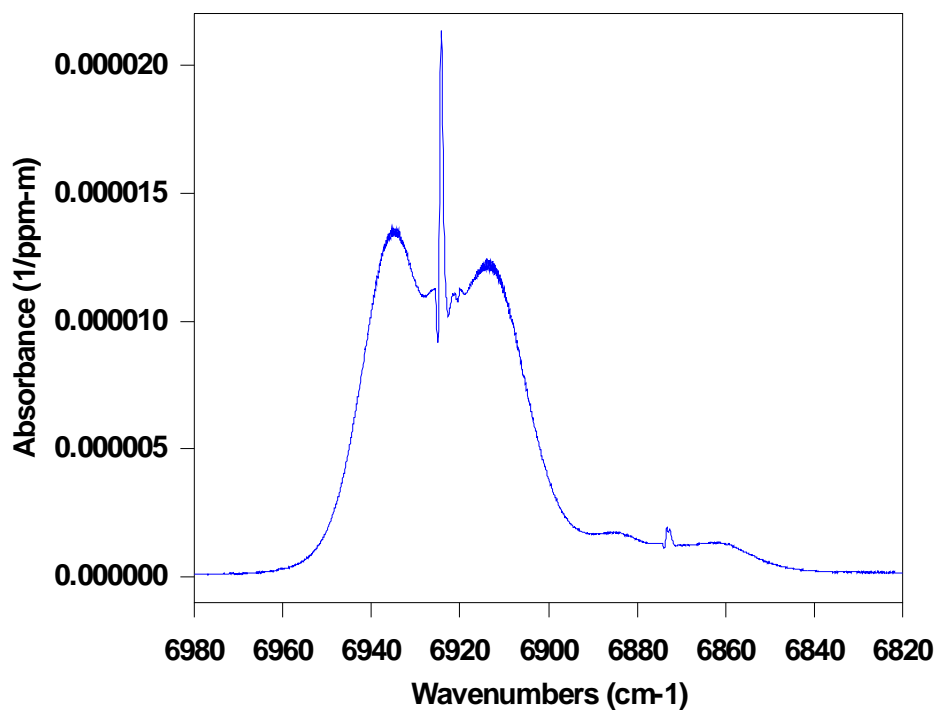


Figure 2. Expanded view of the  $2\nu_{24}$  first N-H overtone band of pyrrole. Even though the spectrum was measured at 760 Torr with  $1\text{ cm}^{-1}$  resolution, the fringe-like structure on the P and R branches indicate that many lines could be targeted in low pressure cavity ring down measurements.

are shown in detail in Figure 2. It is interesting to note that even though the spectrum was measured at 760 Torr with  $1\text{ cm}^{-1}$  resolution, the fringe-like structure on the P and R branches indicate that many lines could be targeted in low pressure cavity ring down measurements. From the spectrum it can be seen that the pyrrole  $2\nu_{24}$  N-H overtone Q band peak transition absorbance is  $2.2 \times 10^{-5}\text{ (ppm m)}^{-1}$  and has a bandwidth  $\sim 17\text{ cm}^{-1}$  (FWHM). The absorbance corresponds to an absorption cross section of  $2.1 \times 10^{-20}\text{ cm}^2\text{ molecule}^{-1}$ . This is, to our knowledge, the first quantitative measurement of the pyrrole N-H overtone absorption cross section.

The pyridine near-infrared gas-phase spectrum is also displayed in Figure 1. The pyridine spectrum is much sparser than that seen for pyrrole and the bands in the shortwave region ( $\sim 4000 - 7000\text{ cm}^{-1}$ ) do not have quite the sharp structure as was seen with pyrrole N-H overtone. Two transitions can be seen, one at around  $4600\text{ cm}^{-1}$  and the other around  $6000\text{ cm}^{-1}$ . The first transition, which is blown up and shown in Figure 3, is a series of combination bands, corresponding to  $\nu(\text{CH}) + \text{Pyr}(8a)$ ,  $\nu(\text{CH}) + \text{Pyr}(8b)$ ,  $\nu(\text{CH}) + \text{Pyr}(19a)$ , and  $2\text{Pyr}(8b) + \text{Pyr}(1)$ , as per the assignments given by Van Meervelt et al.<sup>62</sup> The second transition, which is blown up and shown in Figure 4, consists of 3 bands that include 1) a combination of aryl ring 2,6 and 3,5 C-H stretch fundamentals, and 2) the first overtones of the 2,6 and 3,5 aryl ring C-H stretches.

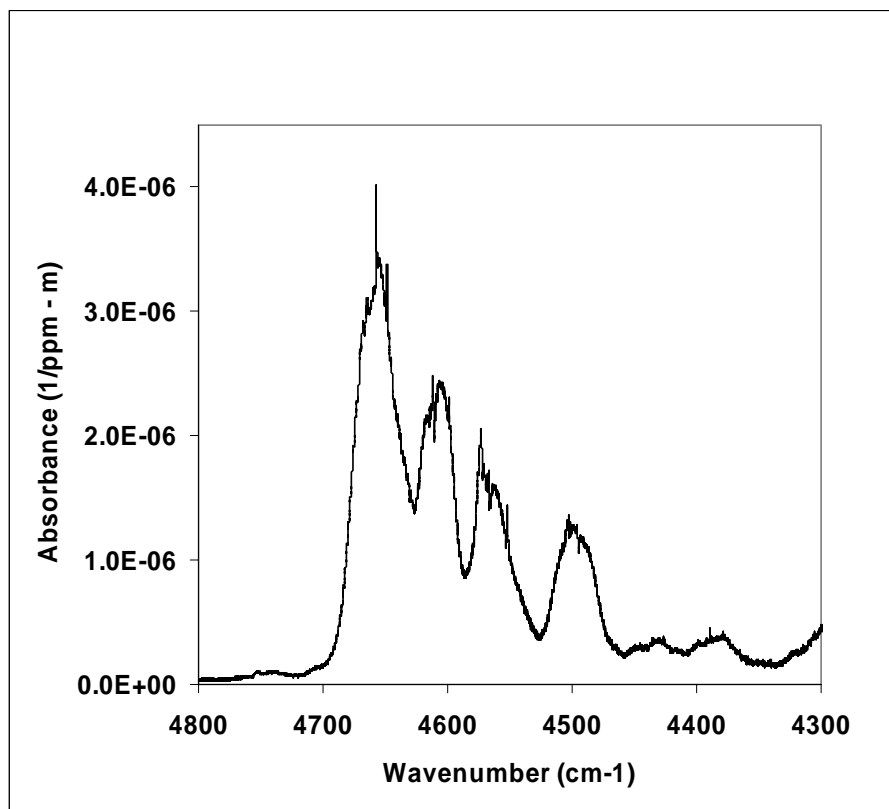


Figure 3. SWIR spectra of the combination bands associated with the pyridine  $\nu(\text{CH}) + \text{Pyr}(8a)$ ,  $\nu(\text{CH}) + \text{Pyr}(8b)$ ,  $\nu(\text{CH}) + \text{Pyr}(19a)$ , and  $2\text{Pyr}(8b) + \text{Pyr}(1)$  vibrations.

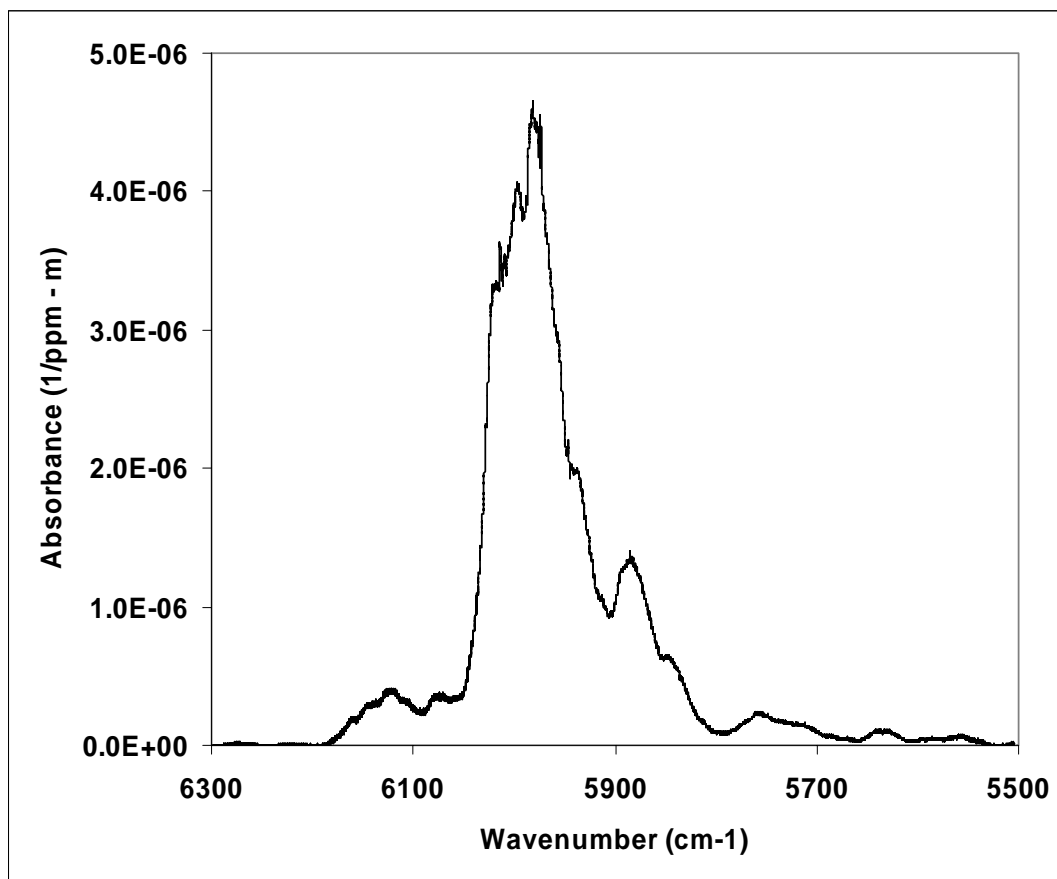


Figure 4. SWIR spectra of pyridine 2,6 and 3.5 CH stretch combination band, and 2,6 and 3,5 C-H stretch first overtones.

While most of the SWIR bands seen for pyridine are associated with C-H stretches, the spectra are unique enough that these bands could be used to positively confirm this molecule's presence, even in the presence of other hydrocarbon species. The peak absorbances observed in the 4600 and 6000  $\text{cm}^{-1}$  regions are  $4 \times 10^{-6}$  and  $4.6 \times 10^{-6} \text{ ppm}^{-1} \text{ m}^{-1}$ , respectively. These correspond to absorption cross sections of  $3.7 \times 10^{-21}$  and  $4.3 \times 10^{-21} \text{ cm}^2 \text{ molec}^{-1}$ , also respectively.

### 6.3 Estimated SWIR CRDS Detection Sensitivity for Pyrrole and Pyridine Biomarkers

PNNL has built and fielded a SWIR CRDS system which is described in detail in Williams et al., 2002, 2003, 2004 and 2005.<sup>63-66</sup> The system detection sensitivity limits for ammonia have been determined to be 0.5 ppmv at 335 Torr operating pressure using the absorption line at  $6528.76 \text{ cm}^{-1}$ . This corresponds to a molecular detection sensitivity of  $5.75 \times 10^{12} \text{ molec cm}^{-3}$ . The absorbance for this line at 1 atm pressure (so that comparison with spectroscopy results for pyridine and pyrrole is relevant) is  $1.21 \times 10^{-5} \text{ ppm}^{-1} \text{ m}^{-1}$  which corresponds to an absorption cross section of  $1.12 \times 10^{-20} \text{ cm}^2 \text{ molec}^{-1}$ . The pyrrole first N-H overtone absorption coefficient was determined to be  $2.1 \times 10^{-20}$  in this study. Since CRDS detection (as measured from the ring down time) scales linearly with absorption cross section and species concentration we can estimate the detection sensitivity for pyrrole to be;

$$\begin{aligned}
[\text{pyrrole}]_{\text{min det}} &= (\sigma_{\text{NH}_3} / \sigma_{\text{pyrrole}}) \times [\text{NH}_3]_{\text{min det}} \\
&= (1.12 \times 10^{-20} / 2.1 \times 10^{-20}) \times 5.75 \times 10^{12} \text{ molec cm}^{-3} \\
&= 3 \times 10^{12} \text{ molec cm}^{-3}.
\end{aligned}$$

For pyridine the best detection sensitivity would occur from monitoring the band in the 6000  $\text{cm}^{-1}$  region, here the absorption cross section was determined to be  $4.3 \times 10^{-21} \text{ cm}^2 \text{ molec}^{-1}$ . The SWIR CRDS detection sensitivity for pyridine should therefore be  $1.5 \times 10^{13} \text{ molec cm}^{-3}$ .

## 7.0 SWIR CRDS Feasibility for Detection Biological Agent Pyrolysis Products

PNNL's SWIR CRDS instrument is outfitted with a cavity that has a volume of  $490 \text{ cm}^3$ . If it is assumed that a sampling apparatus could be designed such that all gas phase products from biological agent pyrolysis would be swept into a prior evacuated CRDS cavity, then the amount of pyrrole and pyridine that needs to come from pyrolysis in order to be detected is  $1.47 \times 10^{15}$  and  $7.35 \times 10^{15}$  molecules, respectively.

There is very little quantitative information on pyrolysis yields of particular chemicals from particular biological species. Most of the published studies on the pyrolysis of bacterial spores have not chemically identified all of the pyrolysis products, reactions, and reactants that are involved in the production of biomarkers. Typically there have been only superficial investigations of particular target compounds and there is, to our knowledge, no data relating observed biomarker signals (i.e. GC, MS, IMS, etc.) to absolute concentrations. Schmidt et al.<sup>35</sup> have reported that their particular pyrolysis apparatus is capable of converting 0.28% of *Escherichia coli* bacterial mass into a gas chromatographic/flame ionization detector response. We will take this as a lower limit for conversion, since this figure does not account for instrument response to different chemicals and necessarily includes loss of gas phase pyrolysate to the GC capillary walls. Fractional pyrolysis yields of pyridine and pyrrole have also not been determined for whole bacterial species. Kuckuk et al. have reported that pyrrole accounts for 0.5% of the gas produced when humus is pyrolyzed.<sup>67</sup> Since humus is expected to contain far less protein (the major source of the pyrrole pyrolysis product) than bacterial spores, we will take this as a lower limit for the production of both pyrrole and pyridine. Another important source for pyridine is the pyrolysis of dipicolinic acid, which comprises 5 = 15% of dry spore weight, but we will ignore this here since we are doing a conservative estimate.

For every microgram of biological spore sample put into a pyrolysis chamber, and assuming that all the gas phase effluent is flown into the SWIR CRDS cavity, the amount of pyrrole or pyridine produced will be;

$$\begin{aligned}
1 \mu\text{g biological sample} \times 0.0028 \text{ pyrolysis} \times 0.005 \text{ fraction gas phase products} &= 1.4 \times 10^{-11} \text{ g} \\
= 1.4 \times 10^{-11} \text{ g} / 67.09 \text{ g/mol} \times 6.022 \times 10^{23} \text{ molec/mol} &= 1.256 \times 10^{11} \text{ molecules.}
\end{aligned}$$

This number is 4 orders magnitude below the estimated SWIR CRDS pyrrole and pyridine detection sensitivities which are  $1.47 \times 10^{15}$  and  $7.35 \times 10^{15}$  molecules, respectively. To generate a detectable amount of pyridine or pyrrole it would therefore be necessary to collect and pyrolysis a 12 mg biological sample. This is far larger than is required for current sensors. It is to be noted that we have used very conservative estimates for the overall pyrolysis efficiency and product fractions, however it is difficult to imagine that these could be changed by a factor of 10,000 by optimizing the pyrolysis conditions. It is therefore concluded that while possible, the large amounts of material required preclude using SWIR CRDS for detecting biological agents at this time.

## 8.0 References

1. Committee on Materials and Manufacturing Processes for Advanced Sensors, National Research Council, "Sensor Systems for Biological Agent Attacks: Protecting Buildings and Military Bases", National Academy Press, 2005.
2. J. P. Fitch, E. Raber and D. R. Imbro, "Technology Challenges in Responding to Biological or Chemical Attacks in the Civilian Sector", *Science*, 302 (5549), 1350 – 1354, (2003).
3. J. P. Fitch et al., *Proc. IEEE* 90, 1708 (2002).
4. A.D. Sappey and E.S. Hill, "Fixed-frequency cavity ringdown diagnostic for atmospheric particulate matter", *Optics Letters* 23, 954 – 956 (1998)
5. J.D. Smith and D.B. Atkinson, "A portable pulsed cavity ring-down transmissometer for measurement of the optical extinction of the atmospheric aerosol", *Analyst* 126(8), 1216 – 1220 (2001).
6. V. Bulatov, M. Fisher and I.Schechter, "Aerosol Analysis by cavity-ring-down spectroscopy", *Anal. Chim. Acta* 466, 1 – 9 (2002).
7. A.W. Strawa, R. Castaneda, T. Owano, D.S. Baer and B.A. Paldus, "The Measurement of Aerosol Optical Properties Using Continuous Wave Cavity Ring-Down Techniques", *Journal of Atmospheric and Oceanic Technology* 20, 454 – 463 (2003).
8. J.E. Thompson, H.D. Nasajpour, B.W. Smith and J.D. Winefordner, "Atmospheric Aerosol Measurements by Cavity Ringdown Turbidimetry", *Aerosol Sci. and Tech.* 37, 221 – 230 (2003).
9. A. Pettersson and E.R. Lovejoy, "Measurement of aerosol optical extinction at 532 nm with pulsed cavity ring-down spectroscopy", *J. Aerosol Science* 35, 995 – 1011 (2004).
10. A.A. Riziq, C. Erlick, E. Dinar and Y. Rudich, "Optical properties of absorbing and non-absorbing aerosols retrieved by cavity ring down (CRD) spectroscopy", *Atmos. Chem. Phys. Discuss*, 6 12347 – 12387 (2006).
11. V. Bulatov, Y. Chen and I. Schechter, "Absorption Characterization of Aerosols by Cavity Ring Down Technique", in *Laser Applications to Chemical, Security and Environmental Analysis*, Technical Digest (Optical Society of America, 2006), paper TuC4.
12. B.A. Richman, A.A. Kachanov and B.A. Paldus, "Novel detection of aerosols: combined cavity ring-down and fluorescence spectroscopy", *Optics Express* 13(9), 3376 – 3388 (2005).
13. D. Naumann, "FT-IR and FT-NIR Raman Spectroscopy in Biomedical Research" in *Fourier Transform Spectroscopy: 11<sup>th</sup> International Conference*, vol 430, J.A. DeHaseth, Ed. Woodbury, NY: AIP 1998, pp. 96 – 109.

14. R. Goodacre, E.M. Timmins, P.J. Rooney, J.J. Rowland and D.B. Kell, "Rapid identification of *Streptococcus* and *Enterococcus* species using diffuse reflectance-absorbance Fourier transform infrared spectroscopy and artificial neural networks", *FEMS Microbiology Letters*, 140, 233 – 239 (1996).
15. N. S. Foster, S. E. Thompson, N. B. Valentine, J. E. Amonette, T. J. Johnson, "Identification of sporulated and vegetative bacteria using statistical analysis of Fourier transform mid-infrared transmission data", *Applied Spectroscopy*, 58, 203 (2004).
16. S.E. Thompson, N.S. Foster, T.J. Johnson, N.B. Valentine and J.E. Ammonette, "Identification of Bacterial Spores Using Statistical Analysis of Fourier Transform Infrared Photoacoustic Spectroscopy Data", *Applied Spec.* 57 (8), 893 – 899 (2003).
17. K.C. Schuster, F. Mertens, J. R. Gapes, "FTIR spectroscopy applied to bacterial cells as a novel method for monitoring biotechnological processes", *Vibrational Spectroscopy* 19, 467 – 477 (1999). – Monitored amide bands and CH stretch regions – relative heights gave an indication of progress and pathway of fermentation process.
18. K.P. Gurton, D. Ligon, and R. Dahmani, "Measured infrared optical cross sections for a variety of chemical and biological aerosol simulants", *Applied Optics* 43(23) 4564 – 4570 (2004). – looked at *Bacillus subtilis* endospores, lyophilized ovalbumin, polyethylene glycol, dimethicone (SF-6), kaolin, Arizona road dust and diesel soot.
19. K.P. Gurton, D. Ligon, and R. Kvavilashvili, "Measured infrared spectral extinction for aerosolized *Bacillus subtilis* var. *niger* endospores from 3 to 13 mm", *Applied Optics*, 40(25) 4443 - 4448 (2001)
20. B.G. Osborne, "Near-infrared Spectroscopy in Food Analysis" in *Encyclopedia of Analytical Chemistry*, R.A. Meyers, Ed., John Wiley & Sons, New York 2000, pp 1 – 14,
21. E. T. Arakawa, P. S. Tuminello, B. N. Khare and M. E. Milhan, "Optical Properties of *Erwinia herbicola* Bacteria at 0.19 – 2.5 mm", *Biopolymers (Biospectroscopy)* 72, 391 (2003).
21. P. S. Tuminello, E. T. Arakawa, B. N. Khare, J. M. Wrobel, M. R. Query and M. E. Milhan, "Optical Properties of *Bacillus subtilis* Spores from 0.2 to 2.5 mm", *Applied Optics*, 36, 2818 (1997).
22. L. E. Rodriguez-Saona, F. M. Khambaty, F. S. Fry and E. M. Calvey, "Rapid Detection and Identification of Bacterial Strains by Fourier Transform Near-Infrared Spectroscopy", *J. Agric. Food Chem.* 49, 574 (2001).
23. P.G. Simmonds, "Whole Microorganisms Studied by Pyrolysis-Gas Chromatography-Mass Spectrometry: Significance for Extraterrestrial Life Detection Experiments", *Appl. Microbio.* 20 (4), 567 – 572 (1970).



24. Smith, P.R., "Generation of Biomarkers from Anthrax Spores by Catalysis and Analytical Pyrolysis", MS Thesis, Department of Chemical Engineering. 2005, Brigham Young University.
25. Beverly, M.B., et al., "A rapid approach for the detection of dipicolinic acid in bacterial spores using pyrolysis/mass spectrometry", *Rapid Communications in Mass Spectrometry*, 10, 455-458 (1996).
26. Morgan, S.L., et al., "Identification of Chemical Markers for Microbial Differentiation and Detection by Gas Chromatography-Mass Spectrometry", in *Modern Techniques for Rapid Microbiological Analysis*, p. 1-18 (1991).
27. Schulten, H.R. and H.D. Beckey, "High Resolution Field Ionization Mass Spectrometry of Bacterial Pyrolysis Products", *Analytical Chemistry*, 45(1), 191-195 (1973).
28. Timmins, E.M. and R. Goodacre, "Rapid quantitative analysis of binary mixtures of *Escherichia coli* strains using pyrolysis mass spectrometry with multivariate calibration and artificial neural networks", *J Appl Microbiol.* , 83(2), 208-18 (1997).
29. Voorheas, K.J., S.J. Deluca, and A. Noguerola, "Identification of Chemical Biomarker Compounds in Bacteria and Other Biomaterials by Pyrolysis Tandem Mass- Spectrometry", *Journal of Analytical and Applied Pyrolysis*, 24, 1-21 (1992).
31. Eudy, L.W., et al., "Gas chromatographic-mass spectrometric determination of muramic acid content and pyrolysis profiles for a group of gram-positive and gram-negative bacteria", *Analyst*, 110(4): p. 381-385 (1985).
32. Snyder, P.A., et al., "Correlation of Mass Spectrometry Identified Bacterial Biomarkers from a Fielded Pyrolysis-Gas Chromatography-Ion Mobility Spectrometry Biotector with the Microbiological Gram Stain Classification Scheme", *Anal. Chem.*, 76, 6492-6499 (2004).
33. A.P. Synder et al., "Field Detection of Bacillus Spore Aerosols with Stand-Alone Pyrolysis-Gas Chromatography-Ion Mobility Spectrometry", *Field Anal. Chem. and Tech.* 3(4-5), 315 - 326 (1999).
34. R. Goodacre et al., "Detection of the Dipicolinic Acid Biomarker in Bacillus Spores Using Curie-Point Pyrolysis Mass Spectrometry and Fourier Transform Infrared Spectroscopy", *Anal. Chem.* 72, 119 = 127 (2000).
35. H. Schmidt et al. "Quantitative assessment and optimization of parameters for pyrolysis of bacteria with gas chromatographic analysis", *J. Anal. & Appl. Pyrolysis*, 76, 161 - 168 (2006).
36. M. D. Krebs et al., "Detection of Biological and Chemical Agents Using Differential Mobility Spectrometry (DMS) Technology", *IEEE Sensors Journal*, 5 (4), 696 - 672 (2005).
36. C. D. Mowry et al., "Miniature Sensors for Biological Warfare Agents using Fatty Acid Profiles: LDRD 10775 Final Report, SAND2003-0168, January 2003.

37. J. P. Dworzanski et al. "Novel biomarkers for Gram-type differentiation of bacteria by pyrolysis-gas chromatography-mass spectrometry", *J. Anal. & Appl. Pyrolysis*, 73 (1), 29 - 38 (2005).
38. P.A. Synder et al., "Orthogonal analysis of mass and spectral based technologies for the field detection of bioaerosols", *Anal. Chim. Acta* 513, 365 - 377 (2004).
39. S. Deluca et al., "Direct Analysis of Bacterial Fatty Acids by Curie-Point Pyrolysis Tandem Mass Spectrometry", *Anal. Chem.* 62, 1465 - 1472 (1990).
40. D. P. Glavin et al., "New Method for Estimating Bacterial Cell Abundances in Natural Samples by Use of Sublimation", *Appl. Env. Microbiology* 70 (10), 5923 - 5928 (2004).
41. Brock, T.D., et al., *Metabolism, Biosynthesis, and Nutrition*, in *Biology of Microorganisms*, T.D. Brock, et al., Editors. 1994, Prentice Hall: Englewood Cliffs.
42. Henriques, A.O. and C.P. Moran, *Methods: Structure and Assembly of the Bacterial Endospore Coat* Vol. 20. 2000: Academic Press Inc. 95-110 (2000).
43. Murrell, W.G., "Chemical Composition of Spores and Spore Structures", in *The Bacterial Spore*, G.W. Gould and A. Hurst, Editors. 1969, Academic Press, Inc., New York.
44. Murrell, W.G., "The Biochemistry of the Bacterial Endospore", in *Advances in Microbial Physiology*, p. 133-251 (1967).
45. Keynan, A. and N. Sandler, "Spore Research in Historical Perspective", in *The Bacterial Spore*, G.W. Gould and A. Hurst, Editors. 1969, Academic Press Inc., New York.
46. Driks, A., "Bacillus subtilis Spore Coat", *Microbiology and Molecular Biology Reviews*, March, 1-20 (1999).
47. Gould, G.W. and A. Hurst, *The Bacterial Spore*. Vol. 1. 1969, New York: Academic Press Inc.
48. H. G. Kjaergaard et al., "CH Stretching Overtone Investigation of Relative CH Bond Lengths in Pyridine", *J. Phys. Chem.* 100, 19273 - 19279 (1996).
49. K. L. McNesby et al., "High-sensitivity laser absorption measurements of broadband absorbers in the near-infrared spectral region", *Appl. Opt.* 39 (27), 5006 - 5008 (2000).
50. A. Mellouki et al., "Spectroscopic investigation of ground state pyrrole: the N-H stretch", *Chem. Phys.* 220, 311 - 322 (1997).
51. Chu, P.M., Guenther, F.R., Rhoderick G.C., and Lafferty, W.J.: *The NIST Quantitative Infrared Database*, *J. Res. Natl. Inst. Stand. Technol.*, **104**, 59, 1999.

52. Sharpe, S.W., Johnson, T.J., Sams, R.L., Chu, P.M., Rhoderick, G.C., and Johnson, P.A.: Gas-phase Databases for Quantitative Infrared Spectroscopy, *Appl. Spectr.*, **58(12)**, 1452-1461, 2004.
53. Sharpe, 2003 Error Analysis
54. Johnson, T.J., Sharpe, S.W. and Covert, M.A., “Disseminator for Rapid, Selectable and Quantitative Delivery of Low and Semivolatile Liquid Species to the Vapor Phase,” *Rev. Sci. Instr.* **77**, 094103, (2006). And also Erratum thereto. *Rev. Sci. Instr.* **78**, 019902, (2007).
55. Johns, J.W. “Thermal artifacts in mid- to far-IR FT spectroscopy”, in *Fourier Transform Spectroscopy: New Methods and Applications*, Vol. 4, 26-27, OSA Technical Digest Series, Optical Society of America, Washington DC, (1995).
56. Birk, M., Hausamann, D., Wagner G., and Johns, J.W.: Determination of Line Strengths by Fourier-transform Spectroscopy, *Appl. Opt.* **35**, 2971-2985, (1996).
57. Johnson, T.J., Sams, R.L., Blake, T.A., Sharpe, S.W., and Chu, P.M.: Removing Aperture-Induced Artifacts from FTIR Intensity Values, *Appl. Opt.* **41**, 2831-2839, 2002.
58. Maki A, Blake TA, Sams RL, Frieh J, Barber J, Masiello T, Chrysostom ETH, Nibler JW, Weber A, “Analysis of some combination-overtone infrared bands of (SO<sub>3</sub>)-S-32-O-16”, *J. Molecular Spec.* 225 (2): 109-122 ( 2004)
59. Johnson, T.J., Valentine, N.B., and Sharpe, S.W.: Mid-infrared versus Far-infrared (THz) Relative Intensities of Room-temperature *Bacillus* spores, *Chem. Phys. Lett.*, **403**, 152-157, 2005.
60. A. Held and M. Herman, “High-Resolution Spectroscopic Study of the First Overtone of the N-H Stretch and of the Fundamentals of the C-H Stretches in Pyrrole”, *Chem. Phys.* 190 (2-3), 407 – 417 (1995).
61. C. Douketis and J.P. Reilly, “The NH stretch in pyrrole – A study of the fundamental and 3<sup>rd</sup> overtone bands in the bulk gas and in a molecular beam”, *J. Chem. Phys.* 96 (5), 3431 – 3440 (1992).
62. L. Van Meervelt, C. Bruyneel, H. Morisse and Th. Zeegers-Huyskens, “X-Ray and Vibrational Studies of the Complex between N-tert-Butoxycarbonyl-L-Phenylalanine and Pyridine: Isotope Effect”, *J. Physical Organic Chem.* 10, 825 – 834 (1997).
63. Williams RM., “Ultra-trace Absorption Measurements Using SWIR Cavity Ringdown Spectroscopy “, PNNL-13974, Pacific Northwest National Laboratory, Richland, WA, 2002.
64. Williams RM, WW Harper, PM Aker, JS Thompson, and TL Stewart, “Chemical Sensing Using Infrared Cavity Enhanced Spectroscopy: Short Wave Infrared Cavity Ring Down

Spectroscopy (SWIR CRDS) Sensor”, PNNL-14475, Pacific Northwest National Laboratory, Richland, WA, 2003

65. Williams RM, JS Thompson, TL Stewart, MS Taubman, BD Cannon, TL Myers, and PM Aker, "Progress in Cavity Enhanced Infrared Sensing." PNNL-SA-41014, Pacific Northwest National Laboratory, Richland, WA, 2004.

66. Williams RM., "Near-infrared cavity-enhanced in situ sensing of molecular signatures of nuclear proliferation." PNNL-SA-44782, Pacific Northwest National Laboratory, Richland, WA, 2005.

67. R. Kuckuk, W. Hill, P. Burba and A.N. Davies, "Pyrolysis-GC-FTIR for structural elucidation of aquatic humic substances", *Fresenius J. Anal. Chem.*, 350, 528 – 532 (1994).